

Fluctuation ratios in the absence of microscopic time reversibility

Sven Dorosz and Michel Pleimling

Department of Physics, Virginia Polytechnic Institute and State University, Blacksburg, Virginia 24061-0435, USA

(Received 24 November 2008; published 12 March 2009)

We study fluctuations in diffusion-limited reaction systems driven out of their stationary state. Using a numerically exact method, we investigate fluctuation ratios in various systems which differ by their level of violation of microscopic time reversibility. Studying a quantity that for an equilibrium system is related to the work done to the system, we observe that under certain conditions oscillations appear on top of an exponential behavior of transient fluctuation ratios. We argue that these oscillations encode properties of the probability currents in state space.

DOI: 10.1103/PhysRevE.79.030102

PACS number(s): 05.40.-a, 05.20.-y, 05.70.Ln

In recent years the study of fluctuations in nonequilibrium small systems has evolved into a very active field of research, see, e.g., Refs. [1–18]. Various fluctuation and work theorems have been formulated and their applicability has been verified in recent experiments [12–18], demonstrating their usefulness for characterizing out-of-equilibrium systems. It is remarkable that these fluctuation relations yield very generic statements valid for large classes of nonequilibrium systems.

Diffusion-limited systems with irreversible reactions form an important class of systems that have not been studied thoroughly in the context of fluctuation relations. In the past all discussed extensions of fluctuation theorems to nonequilibrium systems with chemical reactions [19–25] focused on reversible reactions and reaction networks. Effectively, however, irreversible reactions can be encountered if the products of the reactions are evacuated rapidly enough. What makes irreversible reactions so interesting is that there is a major qualitative difference with reversible reactions: whereas in the latter case microscopic time reversibility holds, in irreversible reaction-diffusion systems microscopic time reversibility is usually broken. As we show in this Rapid Communication the absence of microscopic reversibility leads to unexpected and nontrivial modifications of the properties of transient fluctuations.

Systems with broken microscopic time reversibility are readily found in granular matter. It has been claimed [26] that fluctuations in fluidized granular medium are in accord with the Gallavotti and Cohen fluctuation theorem. As the fluctuation theorem requires microscopic reversibility, this interpretation of the experimental data is problematic and has been criticized [27]. However, in [28] it has been proposed that under certain assumptions and for a specific time scale a fluctuation relation should be recovered in granular materials. In our study we will not be able to contribute directly to this controversy, but the results presented in this Rapid Communication clearly show the interesting and nontrivial character of fluctuations in systems in which microscopic reversibility is absent.

In diffusion-limited reaction systems the stationary states can be true nonequilibrium states. Due to their relative simplicity, in conjunction with a highly nontrivial physical behavior, reaction-diffusion systems are considered to be paradigmatic examples of nonequilibrium many-body systems. Thus our current understanding of nonequilibrium phase

transitions [29] and of aging phenomena in absence of detailed balance [30] has mainly emerged through numerous studies of the out-of-equilibrium behavior of these systems.

We consider here one-dimensional lattices of N sites with periodic boundary conditions. Forbidding multiple occupancy of a given lattice site, particles A jump to unoccupied nearest-neighbor sites with a diffusion rate D and undergo various reactions. We discuss in the following three different reaction schemes, see Table I, and we denote with model 1, 2, and 3 the three models that result from these reaction schemes. Obviously, the reactions change the number of particles in the system, whereas the diffusion keeps the particle number constant.

For fixed values of the reaction and diffusion rates, model 1 is in (chemical) equilibrium. This is different for the other two models where microscopic reversibility is partly or fully broken. By breaking microscopic reversibility we mean that if $\omega(C \rightarrow C')$ is the transition probability from configuration C to configuration C' , we can have the situation that $\omega(C \rightarrow C')=0$ even though $\omega(C' \rightarrow C)>0$. For model 2 we observe that some reactions are reversible whereas others are not. For example, whereas we can create a new particle in the middle of two empty sites, $000 \rightarrow 0A0$ with rate h , it is not possible to directly go back to the configuration with three empty sites by destroying this isolated A particle, as we need to have two neighboring A particles for particle annihilation. This is different for $00A \rightarrow 0AA$, as here a direct path back to the initial configuration exists. Finally, in model 3 microscopic reversibility is broken for all reactions.

We can readily access the stationary probability distributions, i.e., the probabilities $P_s(C_i)$ to encounter the microscopic configuration C_i in a given stationary state. This is done in the usual way by rewriting the master equations in

TABLE I. The three reaction schemes discussed in this Rapid Communication. A new particle can only be created at an empty lattice site.

Model 1	Model 2	Model 3
$A+A \xrightarrow{\lambda} 0+A$	$A+A \xrightarrow{\lambda} 0+A$	$A+A \xrightarrow{\lambda} 0+0$
$A+0 \xrightarrow{h} A+A$	$0 \xrightarrow{h} A$	$0 \xrightarrow{h} A$

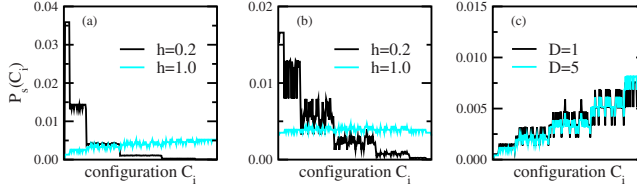


FIG. 1. (Color online) Stationary probability distributions for (a) model 1 with $\lambda=1$ and $D=1$, (b) model 3 with $\lambda=1$ and $D=1$, and (c) model 2 with $\lambda=1$ and $h=1.4$. Shown are the distributions for two values of the creation rate h , respectively, of the diffusion constant D , for systems with $N=8$ lattice sites. The configurations are grouped by number of particles.

matrix form involving the Liouvillian and by noticing that the stationary probabilities form the unique eigenvector of this operator to the eigenvalue 0. With N sites we have 2^N configurations as there is at most one particle on each lattice site. The null eigenvector of the resulting $2^N \times 2^N$ matrix is obtained using standard algorithms. Figure 1 shows the stationary probability distributions for three different cases. Configurations with the same number of particles are grouped, with the empty configuration to the left and the fully occupied lattice to the right. When the creation of new particles takes place with a small rate, see Figs. 1(a) and 1(b), the most probable configurations are those with few occupied sites, whereas the configurations with more occupied sites have an increasing weight for increasing creation rates. Similar changes are observed when changing the rate λ . Obviously, a change of reaction rates has a large impact on the stationary probability distributions. This is different for the diffusion constant D which only changes the distributions quantitatively and not qualitatively, as shown in Fig. 1(c). We remark that even though there are visible differences in the stationary probability distributions, it is far from obvious how one should infer from these distributions the equilibrium (model 1) or strongly nonequilibrium (model 3) nature of the system.

In order to obtain a better understanding of our systems we look at the transient behavior when we drive the system from one stationary state to another by changing a reaction rate. Experimentally, a change of rates in chemical reactions can be achieved by changing the temperature. In our protocol we change one of the rates r from an initial value r_0 to a final value r_M in M equidistant steps of length Δr , yielding the values $r_i = r_0 + i\Delta r$ with $i=0, \dots, M$. We compute the observable [9]

$$\delta\phi = \sum_{i=0}^{M-1} [\ln P_s(C_i, r_{i+1}) - \ln P_s(C_i, r_i)], \quad (1)$$

where $P_s(C_i, r_i)$ is the probability to find the configuration C_i in the stationary state corresponding to the value r_i of the reaction rate r . For a system in thermal equilibrium the quantity $\delta\phi$ is given by $\delta\phi = \beta(W - \Delta F)$, where β is the inverse temperature, W is the work done to the system, and ΔF is the difference between the free energies of the initial and final states. It is important to note that the quantity (1) is still well defined in absence of microscopic reversibility. This is not

the case for many of the quantities that have been studied recently in the context of fluctuation relations.

Hatano and Sasa [9] proved for Langevin systems with continuous dynamics that the quantity (1) fulfills in the limit $M \rightarrow \infty$ the following simple fluctuation relation:

$$\langle e^{-\delta\phi} \rangle = 1, \quad (2)$$

where the average is the average over all possible histories relating the initial and final steady states. For an equilibrium system the relation (2) reduces to the well-known Jarzynski relation [4]. Even though not explicitly stated in [9], the property (2) of $\delta\phi$ can be shown in a straightforward way to also hold in systems with discrete dynamics, and this independently on whether microscopic reversibility prevails or not. The verification of the relation (2) is therefore a very good benchmark in order to validate our numerical approach.

Changing the rate r from the initial value r_0 to the final value r_M in M steps, we can easily compute the exact stationary probability distributions for any value r_i with $i=0, \dots, M$. In order to verify Eq. (2) we need to generate all possible sequences of configurations (*paths* in configuration space) $C_0 \rightarrow C_1 \rightarrow \dots \rightarrow C_{M-1} \rightarrow C_M$, determine the weights $\prod_{i=0}^{M-1} P_s(C_0, r_0) \omega(C_i \rightarrow C_{i+1}, r_{i+1})$ and the values of $\delta\phi$ along the different paths, and average over all these possibilities. Here $\omega(C_i \rightarrow C_{i+1}, r_{i+1})$ is the transition probability from configuration C_i to configuration C_{i+1} at the value r_{i+1} of our reaction rate. With this numerical exact calculation we verify for all studied cases the validity of the integral fluctuation relation (2) with deviations less than 10^{-7} .

As in our numerically exact approach we generate all paths recursively, the CPU time needed for the generation of all trajectories grows exponentially with the lattice size N and the number of steps M , and only rather small system sizes (with $N < 10$) can be accessed in this way. For example, for $N=8$ we generate 2.6×10^8 different trajectories for $M=6$, whereas 2.7×10^{10} trajectories are generated for $M=8$. We also studied larger systems through Monte Carlo simulations and checked that these results are consistent with the numerical exact results obtained for the small systems. For this reason we focus in the following on the numerically exact results and defer a discussion of the Monte Carlo simulations to later [31].

Before discussing the detailed fluctuation relation, let us first look at the probability distribution $P_F(\delta\phi)$ of the quantity $\delta\phi$ for the forward process where the rate r is changed from r_0 to r_M as well as at the probability distribution $P_R(\delta\phi)$ for the reversed process where r is changed from r_M to r_0 . In the reversed process the rate r takes on the same values as in the forward process but in the reversed order. We show in Fig. 2 the resulting probability distributions for the three models with $N=8$ sites where we change the creation rates from $h_0=0.2$ to $h_M=1.4$ in $M=8$ equidistant steps. Interestingly, the probability distributions are skewed distributions that exhibit additional intriguing peaks. Increasing the diffusion rate D leads to a sharpening of these peaks, as is shown in Fig. 3 for model 3 with $M=6$ and different values of D . We checked that the main contributions to these peaks comes from those trajectories in configuration space where diffusion steps abound, whereas reactions, which change the

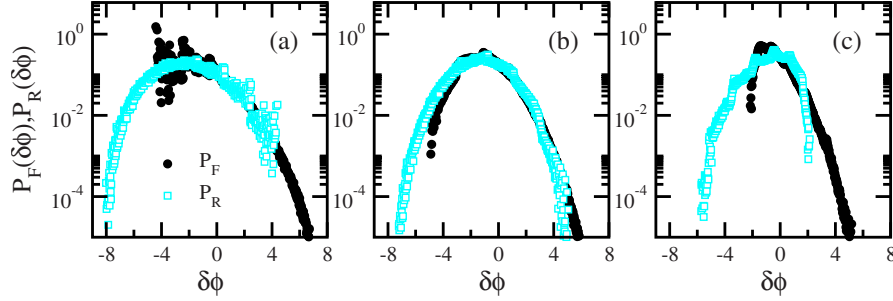


FIG. 2. (Color online) Probability distributions P_F and P_R as a function of $\delta\phi$ for the forward and reversed processes: (a) model 1, (b) model 2, (c) model 3, with $\lambda=1$, $D=1$, and $N=8$. In all cases the rate of particle creation was changed from $h_0=0.2$ to $h_M=1.4$ in $M=8$ steps. The scattering in the data is not due to poor statistics, as we are using a numerical exact method for the computation of the probability distributions.

number of particles in the system, only take place rarely. It should be noted that for very large values of D the peaks also appear for the equilibrium model 1 and are therefore not characteristic of broken microscopic time reversibility.

In Fig. 4 we discuss the fluctuation ratio $P_F(\delta\phi)/P_R(-\delta\phi)$ for the observable (1). For a system that fulfills detailed balance for all values of the rate r we expect that

$$P_F(\delta\phi)/P_R(-\delta\phi) = \exp(\delta\phi). \quad (3)$$

Indeed, it is straightforward to show that for a system initially in thermal equilibrium relation (3) together with the definition (1) of the quantity $\delta\phi$ yields the Crooks relation

$$P_F(W)/P_R(-W) = \exp[\beta(W - \Delta F)]. \quad (4)$$

In order to highlight any deviations from the exponential behavior, we plot in the lower panels of Fig. 4 the quantity $e^{-\delta\phi}P_F(\delta\phi)/P_R(-\delta\phi)$. Looking at Figs. 4(a) and 4(d), we observe that for the equilibrium model 1 the ratio of the two probability distributions indeed displays a perfect exponential behavior. As the probability distributions themselves are skewed distributions, see Fig. 2, this is a nontrivial result that nicely demonstrates the importance of the Crooks relation.

As already discussed, microscopic reversibility is partly broken for model 2: whereas many trajectories in configuration space are fully reversible, this does not hold true for all of them. We observe that the probability distribution ratio still displays an exponential behavior on average, see Fig.

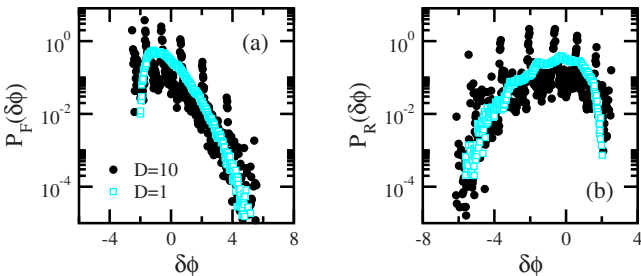


FIG. 3. (Color online) Probability distributions P_F (a) and P_R (b) as a function of $\delta\phi$ for model 3 with $\lambda=1$, $N=8$, and h changing from $h_0=0.2$ to $h_M=1.4$ in $M=6$ steps. The peaks are more pronounced for larger values of D .

4(b), but the data do not fall any more exactly on the exponential curve but instead are scattered around that curve [Fig. 4(e)].

For model 3, where microscopic reversibility is absent, a remarkable change takes place and systematic deviations from the exponential behavior are observed, see Figs. 4(c) and 4(f). These deviations take the form of oscillations. As we argue in the following, these deviations reveal properties of the probability currents in state space.

In order to develop a better understanding for the origin of these oscillations, we studied systematically the dependence of this feature on the reaction and diffusion rates as well as on the system size and the number M of elementary steps [31]. In fact, the oscillations are very robust and are encountered for all studied values of the system parameters. We also observe that a change of the positions of the peaks is directly related to a qualitative change of the stationary probability distributions, as the position of the peaks strongly shifts when the reaction rates are changed, but do only change slightly when the diffusion constant is modified. Changing

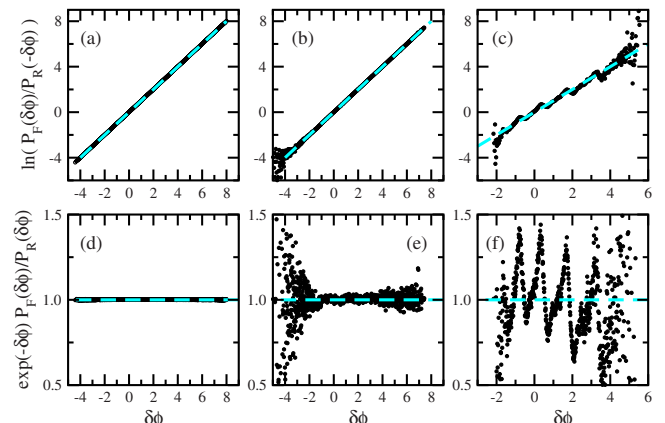


FIG. 4. (Color online) Ratio $P_F(\delta\phi)/P_R(-\delta\phi)$ as a function of $\delta\phi$ for (a) and (d) model 1, (b) and (e) model 2, and (c) and (f) model 3, with $\lambda=1$, $D=1$, $N=8$, and $M=8$, whereas h is changed from $h_0=0.2$ to $h_M=1.4$. In the lower panels we plot $e^{-\delta\phi}P_F(\delta\phi)/P_R(-\delta\phi)$ in order to highlight deviations from the equilibrium behavior (3). The dashed lines indicate the expected behavior (3) for a system in equilibrium before and after the change of parameter.

the diffusion constant, however, greatly enhances the peak height.

At this stage one might think that the peaks observed in the probabilities P_F and P_R , see Figs. 2 and 3, are the origin of the peaks in the probability ratio. On the one hand, there is of course an intimate relation between the peaks in P_F and P_R and those encountered when taking the ratio of these two probabilities. On the other hand, however, peaks also appear in P_F and P_R for models 2 and 1, even though no peaks are observed for the corresponding ratio. The appearance of peaks in the probabilities P_F and P_R is therefore a necessary condition, but it alone cannot explain our observations.

It is important to note that model 3 differs qualitatively from models 1 and 2. For all the models the configuration space is divided into different subspaces, characterized by a constant number of particles in the system, which are invariant under the action of diffusion. A passage from one subspace to the other only takes place when the number of particles is changed by a reaction. In models 1 and 2 every reaction changes the number of particles by one, thus connecting different subspaces pairwise. One of the consequences of this is that the peaks in the distributions P_F and P_R compensate each other when computing the ratio $P_F(\delta\phi)/P_R(-\delta\phi)$. This compensation is only approximate for model 2 due to the fact that some trajectories can not be traveled in the reversed direction when reversing the protocol. The situation is different for model 3 as here we have an asymmetry in the change of particle numbers: whereas the

number of particles is enhanced by one in the creation process, two particles are always destroyed in the annihilation process. Consequently, the trajectories in configuration space for the forward and backward processes are completely different, as they connect the different subspaces with fixed number of particles in a different way. It follows that probability currents for the forward and backward process are also very different. This yields probability distributions P_F and P_R whose peaks do not compensate each other when the ratio is formed, thus giving place to the observed systematic deviations. It is clear from this discussion that we expect this mechanism, and therefore the observed systematic deviations, to be common in systems where the absence of microscopic reversibility is accompanied by an asymmetry in the probability currents in configuration space.

In summary, we have studied reaction-diffusion systems and showed that the absence of microscopic reversibility can lead for transient fluctuation ratios for the observable $\delta\phi$ to systematic deviations from the exponential behavior encountered in systems with equilibrium steady states. These deviations take the form of oscillations, and we argue that this intriguing feature reveals properties of the probability currents in state space.

It is a pleasure to thank Chris Jarzynski, Uwe Täuber, Frédéric van Wijland, and Royce Zia for interesting and helpful discussions.

-
- [1] D. J. Evans, E. G. D. Cohen, and G. P. Morriss, Phys. Rev. Lett. **71**, 2401 (1993).
 - [2] D. J. Evans and D. J. Searles, Phys. Rev. E **50**, 1645 (1994).
 - [3] G. Gallavotti and E. G. D. Cohen, Phys. Rev. Lett. **74**, 2694 (1995).
 - [4] C. Jarzynski, Phys. Rev. Lett. **78**, 2690 (1997).
 - [5] J. Kurchan, J. Phys. A **31**, 3719 (1998).
 - [6] J. L. Lebowitz and H. Spohn, J. Stat. Phys. **95**, 333 (1999).
 - [7] G. E. Crooks, Phys. Rev. E **60**, 2721 (1999).
 - [8] G. E. Crooks, Phys. Rev. E **61**, 2361 (2000).
 - [9] T. Hatano and S.-I. Sasa, Phys. Rev. Lett. **86**, 3463 (2001).
 - [10] S. Mukamel, Phys. Rev. Lett. **90**, 170604 (2003).
 - [11] U. Seifert, Phys. Rev. Lett. **95**, 040602 (2005).
 - [12] J. Liphardt *et al.*, Science **296**, 1832 (2002).
 - [13] D. Collin *et al.*, Nature (London) **437**, 231 (2005).
 - [14] F. Douarche *et al.*, Europhys. Lett. **70**, 593 (2005).
 - [15] G. M. Wang, E. M. Sevick, E. Mittag, D. J. Searles, and D. J. Evans, Phys. Rev. Lett. **89**, 050601 (2002).
 - [16] D. M. Carberry *et al.*, Phys. Rev. Lett. **92**, 140601 (2004).
 - [17] C. Tietz, S. Schuler, T. Speck, U. Seifert, and J. Wrachtrup, Phys. Rev. Lett. **97**, 050602 (2006).
 - [18] J. Berg, Phys. Rev. Lett. **100**, 188101 (2008).
 - [19] P. Gaspard, J. Chem. Phys. **120**, 8898 (2004).
 - [20] U. Seifert, J. Phys. A **37**, L517 (2004).
 - [21] D. Andrieux and P. Gaspard, J. Chem. Phys. **121**, 6167 (2004).
 - [22] U. Seifert, Europhys. Lett. **70**, 36 (2005).
 - [23] D. Andrieux and P. Gaspard, Phys. Rev. E **74**, 011906 (2006).
 - [24] T. Schmiedl and U. Seifert, J. Chem. Phys. **126**, 044101 (2007).
 - [25] D. Andrieux and P. Gaspard, Phys. Rev. E **77**, 031137 (2008).
 - [26] K. Feitosa and N. Menon, Phys. Rev. Lett. **92**, 164301 (2004).
 - [27] A. Puglisi, P. Visco, A. Barrat, E. Trizac, and F. van Wijland, Phys. Rev. Lett. **95**, 110202 (2005).
 - [28] F. Bonetto *et al.*, J. Stat. Mech.: Theory Exp. (2006), P05009.
 - [29] H. Hinrichsen, Adv. Phys. **49**, 815 (2000).
 - [30] M. Henkel, J. Phys.: Condens. Matter **19**, 065101 (2007).
 - [31] S. Dorosz and M. Pleimling (unpublished).